IOPscience iopscience.iop.org

Home Search Collections Journals About Contact us My IOPscience

Interdiffusion in low-temperature annealed amorphous CoMoN/CN compound soft-x-ray optical multilayer mirrors

This article has been downloaded from IOPscience. Please scroll down to see the full text article.

2003 J. Phys.: Condens. Matter 15 1235

(http://iopscience.iop.org/0953-8984/15/8/308)

View the table of contents for this issue, or go to the journal homepage for more

Download details:
IP Address: 171.66.16.119
The article was downloaded on 19/05/2010 at 06:36

Please note that terms and conditions apply.

INSTITUTE OF PHYSICS PUBLISHING JOURNAL OF PHYSICS: CONDENSED MATTER

J. Phys.: Condens. Matter **15** (2003) 1235–1246 PII: S0953-8984(03)56997-1

Interdiffusion in low-temperature annealed amorphous CoMoN/CN compound soft-x-ray optical multilayer mirrors

H L Bai[1,2,3], Q H Guo[1], Z J He[1], W B Mi[1], P Wu[1,2], Z Q Li[1,2] and E Y Jiang[1,2]

[1] Institute of Advanced Materials Physics and Faculty of Science, Tianjin University, Tianjin 300072, People's Republic of China
[2] Key Laboratory for Advanced Ceramics and Machining Technology of Ministry of Education, Tianjin University, Tianjin 300072, People's Republic of China

E-mail: baihaili@public.tpt.tj.cn

Received 2 December 2002
Published 17 February 2003
Online at stacks.iop.org/JPhysCM/15/1235

Abstract

Interfacial interdiffusion in dual-facing-target sputtered amorphous CoMoN/CN soft-x-ray optical multilayer mirrors has been investigated quantitatively by monitoring the enhancement of the first-order modulation peak on annealing in the temperature range of 498–548 K. Smaller negative interdiffusivity is quite noticeable by comparing with those of Co/C and CoN/CN systems, signalling that relatively stable interfaces were formed by incorporation of molybdenum. Thermodynamic calculation reveals that the increase of binding enthalpy is the main factor leading to a larger activation energy and hence the smaller interdiffusion coefficient. The results imply that it is possible to further improve the thermal stability of CoN/CN multilayers by doping with refractory metals such as molybdenum.

1. Introduction

Soft-x-ray optical multilayer mirrors are one-dimensional periodic structures consisting of alternating layers of low- and high-electron-density materials, generally referred to as spacer and absorber respectively. As effective soft-x-ray reflectors, the multilayers have been successfully used in branches of science such as microscopy [1] astronomy [2], lithography [3], imaging [4], spectroscopy [5] and x-ray lasers [6]. The most common spacer materials currently in use are C, B_4C and Si, because of the ease of growing thin films and their stability. Optically, suitable absorbers include Fe, Co, Ni, Ru, W and Mo, which are usually used for

[3] Author to whom any correspondence should be addressed.

0953-8984/03/081235+12$30.00 © 2003 IOP Publishing Ltd Printed in the UK

reflections at different wavelengths, e.g. Co(Ni, Fe, W)/C for 4.5–6.5 nm [4, 7–9], Ru/B_4C for 6.5–12.4 nm [10] and (Mo, B)/Si for 12.4–30 nm [11–13].

With the development of synchrotron optics, soft-x-ray optical multilayers are often used as reflectors under high-brilliance synchrotron radiation beams, which can produce a significant heat load on the mirror, and increase their temperature up to several hundred degrees centigrade. Thus, thermal stability is one of the important factors that must be considered for the soft-x-ray optical multilayers used in high-temperature environments [14–16]. Unfortunately, most soft-x-ray optical multilayer systems are destroyed either due to the recrystallization of the amorphous sublayers or to the interfacial reaction and interdiffusion. We thus need to develop a new generation of soft-x-ray multilayers that can work under a high-power beam without radiation damage. A possible solution to avoiding the occurrence of interdiffusion, sublayer crystallization and interfacial compound formation is to make compound multilayers instead of elemental multilayers. Both the absorber and the spacer can be made of relatively inert and stable compounds so that the tendency of interdiffusion and reaction at the interface is minimized. Another advantage is that compounds are generally deposited in amorphous condition. Their composition can be chosen such that they have a relatively high glass transition temperature.

We have fabricated compound CoMoN/CN soft-x-ray optical multilayers by dual-facing-target sputtering (DFTS), and in this paper will report on the interdiffusion in the low-temperature annealed CoMoN/CN soft-x-ray optical multilayer mirrors. The reason for placing the emphasis on the interfacial diffusion is that the reflection profile will change when the interdiffusion or intermediate-phase formation occurs at the interfaces during annealing, and the optical performance of the multilayer mirrors depends sensitively on the chemical stability of these interfaces [17].

2. Experimental details

The multilayer samples were made by a DFTS system. The typical base pressure of the chamber was better than 1.33×10^{-4} Pa. The targets, 10 cm in diameter, were 99.999% purity C and 99.99% purity Co with 99.99% purity Mo pellets placed symmetrically on it. During the deposition, the total pressure of Ar and N_2 gas was kept at 5.33×10^{-1} Pa, and the ratio of partial pressure of N_2 to Ar was fixed at 0.25. A series of CoMoN/CN multilayers was fabricated on ultra-smooth crystalline (111) silicon wafers and NaCl crystals with a freshly cleaved surface. The nominal structures are periods of 2.5 and 5.0 nm, both with a ratio of the thickness of the CoMoN layer to the multilayer period of $\Gamma = 0.4$. No attempt was made to remove the natural oxide layer on the silicon wafers prior to the deposition.

The samples were annealed in a vacuum furnace at 1.33×10^{-4} Pa pressure. The anneal temperature was controlled within ± 1 K. In order to avoid the sample to sample fluctuation, the annealed sample was cut into pieces with the same shape and area, and each piece was characterized before and after the treatment.

All x-ray diffraction measurements were made using the Cu Kα radiation. Using low-angle x-ray diffraction (LAXRD), the multilayer period Λ was determined with the Bragg equation, modified for refraction [18]

$$\sin^2(\theta_m) = \left(\frac{m\lambda}{2\Lambda}\right)^2 + 2\delta, \tag{1}$$

where Λ is the modulation period, θ the position of the low-angle diffraction peak, m the integer reflection order number and δ the average deviation of the refractive index from unity. Λ can be determined from the linear regression of the $\sin^2\theta_m$ versus m^2 plot.

Standard θ–2θ high-angle x-ray diffraction (HAXRD) was used here to identify the phases present in the as-deposited and annealed CoMoN/CN multilayers. The microstructures of the samples deposited on the NaCl(100) single crystal were investigated by using a JEM-200CX transmission electron microscope (TEM) operated at 200 kV. Selected-area electron diffraction (SAED) and bright-field imaging were employed to characterize the films at various annealing temperatures.

In order to obtain the real atomic fractions of elements in the CoMoN and CN sublayers, we also prepared ~100 nm thick CoMoN and CN monolayers under the identical conditions as the sublayers were fabricated. X-ray photoelectron spectra were then recorded after removing the contaminated surface layer by 2 keV 1 μA mm^{-2} ion beam etching, in a Perkin Elmer PhI 5300 spectrometer (Mg Kα radiation) equipped with a spherical capacitor analyser.

3. Data analyses

The compositionally modulated film technique [19–21] allows the measurement of small interdiffusivities by low-angle x-ray specular reflectivity measurements. The advantages of the technique are that

(1) it is very sensitive, and can measure the interdiffusivities down to 10^{-27} m^2 s^{-1},
(2) it is nondestructive, and this makes it possible to perform time-resolved studies of interdiffusivity with annealing, and
(3) the diffusion process for extremely minute displacements of the diffusing atoms can be revealed by x-ray diffraction.

The disadvantage of this technique is that only chemical interdiffusivity, not the chemical diffusivities of individual species, can readily be extracted.

For the concentration distribution of a multilayer of small amplitude, the composition dependence of the mobility M, the second derivative of the Helmholtz energy f_0'' and gradient energy coefficient k are negligible. The changes of concentration with time can thus be described by the Cahn linear diffusion equation [22, 23]

$$\frac{\partial c}{\partial t} = D\frac{\partial^2 c}{\partial x^2} - \frac{2D}{f_0''}k\frac{\partial^4 c}{\partial x^4}, \tag{2}$$

where c is the concentration variable related to time and $D = Mf_0$ is the macroscopic interdiffusion coefficient. A particular solution to equation (2) is

$$c - c_0 = A(t)\cos\beta x, \tag{3}$$

$$A(t) = A_0 \exp\left[-D\beta^2\left(1 + \frac{2k\beta^2}{f_0''}\right)t\right], \tag{4}$$

where c_0 is the average composition, $A(t)$ is the amplitude of the composition wave at time t and $\beta = 2\pi/\Lambda$. It is clear that the higher-order Fourier components have decayed out during the deposition due to interdiffusion.

A composition modulation produces satellites on higher-angle and on lower-angle sides about each Bragg peak. For the special case of (000) Bragg satellites, the diffracted intensity is proportional to the square of the Fourier transform of the composition variation, i.e.

$$I \propto |A|^2. \tag{5}$$

From equations (4) and (5), the time dependence of all satellites can be expressed as

$$\frac{\mathrm{d}}{\mathrm{d}t}\ln[I(t)/I(0)] = -2D\left(1 + \frac{2k\beta^2}{f_0''}\right)\beta^2 = -2D_\Lambda\beta^2, \tag{6}$$

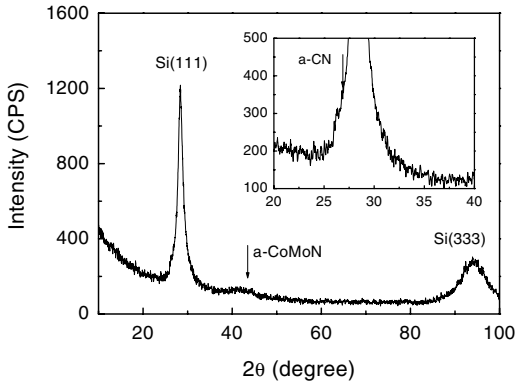

Figure 1. HAXRD pattern of as-deposited 20-layer-pair CoMoN/CN multilayers with a nominal period of 5.0 nm.

Table 1. Relative atomic fractions determined by XPS.

	Atomic fraction (at.%)		
Elements	CoMoN	CN	CoN
C	—	65	—
N	25.6	35	17.4
Co	68.2	—	82.6
Mo	6.2	—	—

where $I(0)$ is the initial intensity and D_Λ the composition and wavelength dependent *effective* interdiffusion coefficient (interdiffusivity). Substituting $\beta = 2\pi/\Lambda$ into equation (6) yields

$$D_\Lambda = -\frac{\Lambda^2}{8\pi^2}\frac{\mathrm{d}}{\mathrm{d}t}\ln[I(t)/I(0)]. \tag{7}$$

Experimentally, within experimental error, $I(0)$ and $I(t)$ in equation (7) can be the integrated or peak intensity. But for convenience, the latter was usually used for the estimation of the interdiffusivity.

4. Results

4.1. Structure characterization

The atomic fractions in the sublayers of CoMoN/CN multilayers can be obtained through the analyses of chemical concentration in the CoMoN and CN monolayers by using XPS. After Ar^+ ion etching, the C XPS peaks related to contamination and the oxygen peak were removed. Thus, the N atomic fractions listed in table 1, calculated using the integrated peak intensity [24] and relative sensitive factors [25], are considered to be the actual chemical composition of the monolayers. Also presented in the table is the N concentration of a CoN monolayer prepared under the same conditions as the CoMoN monolayer was deposited. Obviously, the atomic fraction of N (27.3 at.% without taking Mo into account) from CoMoN films is much higher than that in CoN films, i.e. Mo doping can effectively enhance the incorporation of nitrogen.

HAXRD and TEM analyses, as shown in figures 1 and 2(a), respectively, did not present any evidence on crystallization, signalling that the as-deposited CoMoN/CN is amorphous.

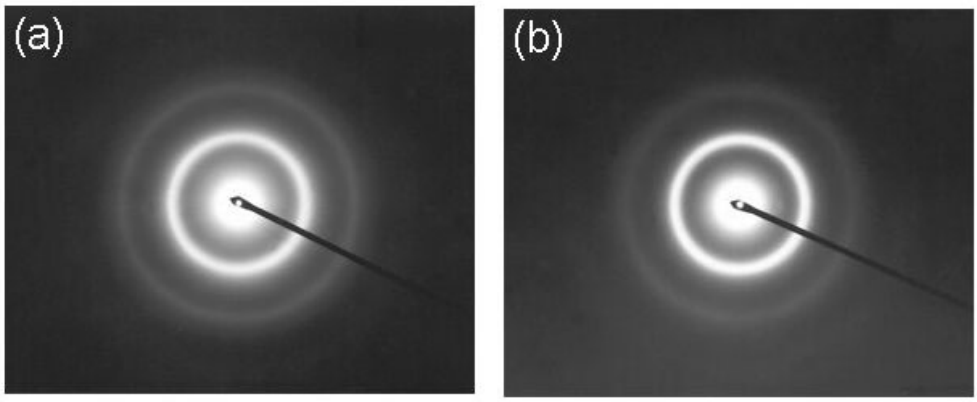

Figure 2. SAED of ten-layer-pair CoMoN/CN multilayers with a nominal period of 5.0 nm, (a) as deposited and (b) annealed at 573 K.

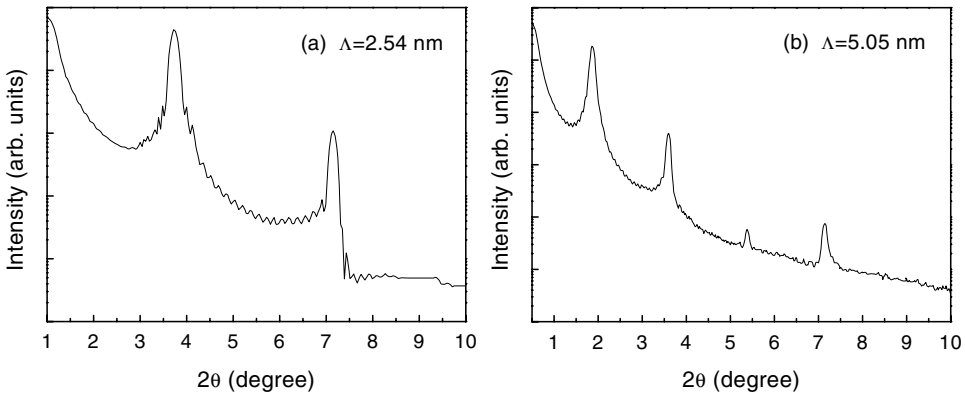

Figure 3. LAXRD patterns of the 20-layer-pair CoMoN/CN multilayers with nominal modulation periods of (a) 2.5 nm and (b) 5.0 nm.

Figures 3(a) and (b) show the LAXRD peaks from the composition modulation of the CoMoN/CN multilayers with nominal modulation periods of 2.5 and 5.0 nm, respectively. The modulation periods Λ derived from the linear plots of $\sin^2\theta_m$ versus m^2 (figure 4) using the modified Bragg law, i.e. equation (1), are 2.54 and 5.05 nm.

4.2. Effective interdiffusivity

TEM annealing analyses, as presented in figure 2, show no crystallization after annealing the ten-layer-pair CoMoN/CN multilayers with periods of 2.54 (not shown) and 5.05 nm for 30 h. Therefore, the influences of sublayer crystallization on the grazing incidence reflectivity that is strongly associated with effective interdiffusivities can be eliminated below 548 K [26–28]. The effective interdiffusivity can thus be determined by monitoring the relative changes in the (000) first-order modulation *peak intensity* $I(t)$, as indicated in equation (7).

Figure 5 shows $\ln[I(t)/I(0)]$ as a function of the annealing time for CoMoN/CN multilayers at three different annealing temperatures. Two regimes, as observed in Co/C and CoN/CN multilayers [29, 30], are also clearly identified from the curves presented in

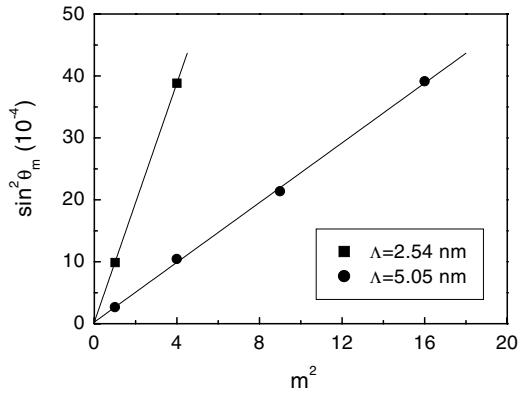

Figure 4. Plots of $\sin^2\theta_m$ versus m^2.

Table 2. Effective interdiffusivities D_Λ of the CoMoN/CN multilayers at different annealing temperatures.

	D_Λ (10^{-24} m^2 s^{-1})		
Λ (nm)	498 K	523 K	548 K
2.54	−0.0807	−0.637	−4.12
5.05	−0.182	−1.53	−10.6

the figure. The rapid initial nonexponential increase (insets of figures 5(a)–(c)) is thought to stem from the interfacial structural relaxation, i.e. short-range diffusion [31]. After the initial structural relaxation, the interdiffusion process reaches the *isoconfigurational condition*; $\ln[I(t)/I(0)]$ is enhanced linearly with the annealing time. By applying equation (2) to the linear regime representing the interdiffusion process, the effective interdiffusivities for the CoMoN/CN multilayers at different annealing temperatures were obtained and are listed in table 2.

4.3. Modulation wavelength dependence of the effective interdiffusivity

The '*effective*' interdiffusivity refers to the fact that the interdiffusion constant is modulation wavelength and concentration dependent. From equation (6), we can further obtain modulation wavelength dependence of the effective interdiffusivity, i.e.

$$D_\Lambda = -\frac{\Lambda^2}{8\pi^2}\frac{\mathrm{d}}{\mathrm{d}t}\ln[I(t)/I(0)] = D\left(1 + \frac{8\pi^2}{\Lambda^2}\frac{k}{f_0''}\right). \tag{8}$$

It is clear that, if there were no *gradient energy effect*, the effective interdiffusion coefficient would be independent of modulation wavelength and equal to the macroscopic interdiffusion coefficient.

Fitting equation (8) to the data listed in table 2, we obtained negative D and k/f_0'', as listed in table 3. Note that $D = Mf_0''$ and M is always positive; the gradient energy coefficient k must be positive, indicating that phase separation occurs at CoMoN–CN interfaces [23].

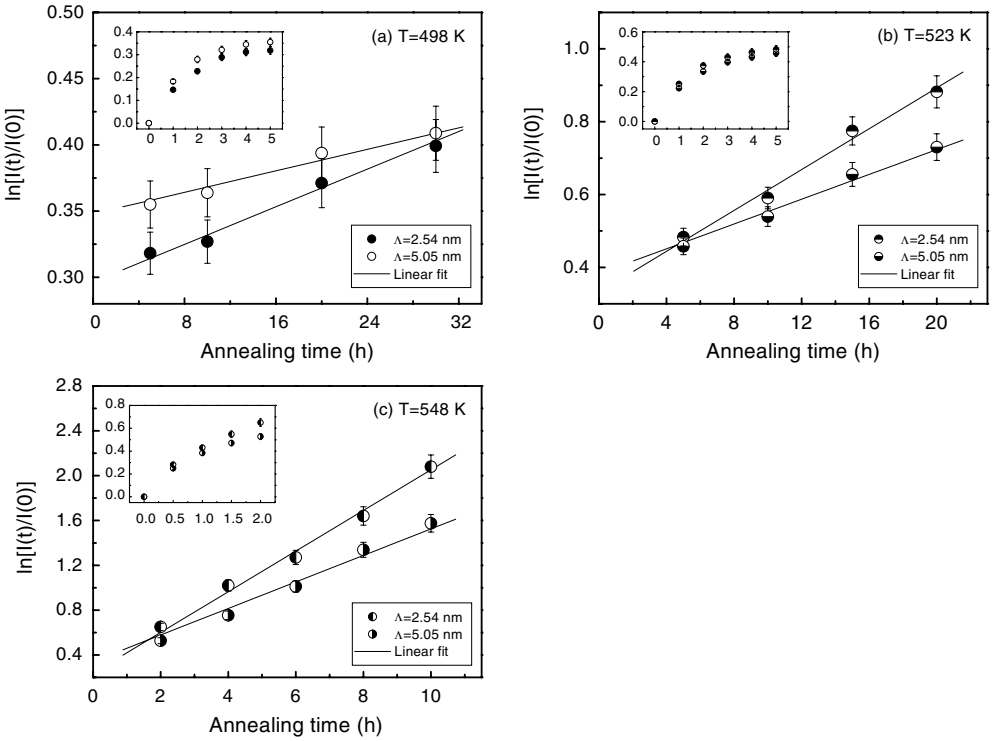

Figure 5. $\ln[I(t)/I(0)]$ as a function of the annealing time for CoMoN/CN multilayers with periods of 2.54 and 5.05 nm at different annealing temperatures, (a) 498 K, (b) 523 K and (c) 548 K.

Table 3. Macroscopic interdiffusion coefficients D and k/f_0'' of the CoMoN/CN multilayers at different annealing temperatures.

T (K)	D (10^{-24} m^2 s^{-1})	k/f_0'' (10^{-20} m^2)
498	−0.216	−5.12
523	−1.83	−5.33
548	−12.8	−5.43

4.4. Temperature dependence of the macroscopic interdiffusion coefficient

In figure 6, $\ln D$ versus $1000/T$ is plotted, indicating the expected temperature dependence of the macroscopic coefficient given by Arrhenius's equation, $D = D_0 \exp(-E/k_B T)$. The temperature dependence of the macroscopic interdiffusion coefficient can thus be determined by linear fitting,

$$D = -5.62 \times 10^{-6} \exp\left[-\frac{(184.9 \pm 23.1)\ \text{kJ mol}^{-1}}{RT}\right]. \tag{9}$$

The activation energy E obtained is 184.9 kJ mol^{-1}, which is larger than that of the CoN–CN system, but still lower than that of self-diffusion of fcc β-Co, 283.4 kJ mol^{-1} [32].

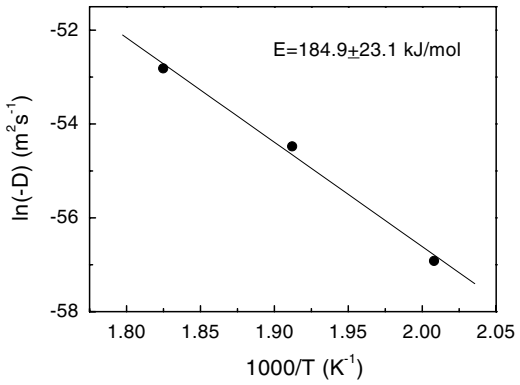

Figure 6. Temperature dependence of the macroscopic interdiffusion coefficient for CoMoN/CN multilayers.

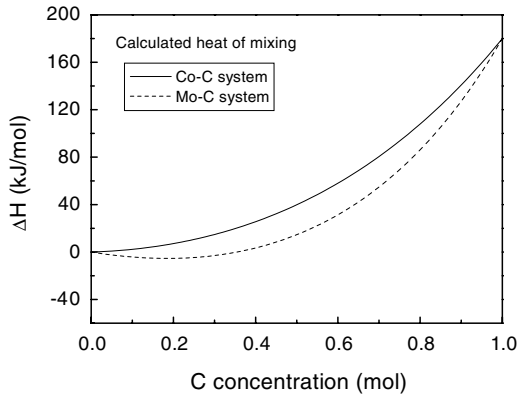

Figure 7. Calculated heat of mixing for Co–C and Mo–C systems.

It is of physical significance to consider which of the constituents dominate the diffusion process. Note that

(1) the x-ray atomic scattering factor of Co is many times larger than those of C and N atoms, and
(2) the atomic fraction of Mo is lower; Co is thought to dominate the changes of the modulation peak intensity, and the measured macroscopic interdiffusion coefficient is primarily concerned with the composition modulation amplitude of Co.

5. Discussions

5.1. On the negative interdiffusivity—thermodynamic consideration

The negative interdiffusivity indicates that the back-diffusion, i.e. phase separation, occurs at the interfaces. According to the regular solution model [23], the gradient energy coefficient $k \propto \Delta H$; ΔH is the enthalpy of mixing and can be written as [33, 34]

$$\Delta H = \Delta H^{ch} + \Delta H^{e}, \tag{10}$$

where ΔH^{ch} is a chemical term given by the model of Miedema *et al* [35, 36]; ΔH^{e} is an elastic contribution due to atomic size mismatch and is always positive. We have calculated

ΔH^{ch} for Co–C and Mo–C systems and found that ΔH^{ch} is always positive for the Co–C system at any composition, as shown in figure 7, while for the Mo–C system ΔH^{ch} shows a small negative value at C composition below 0.35 mol and increases sharply above it. Actually, at CoMoN–CN interfaces, the atomic fraction ratio of Mo to C is believed to be much smaller than 1.86 (0.65/0.35) due to the slight Mo doping. Considering $k \propto \Delta H$ and equation (10), we obtained $k > 0$. Because a positive gradient energy coefficient is characteristic of a phase-separating system, the positive k indicates that Co–C is a phase-separating system, and it is energy favourable for the Mo–C system to separate into two phases at larger C concentration.

5.2. On the smaller interdiffusivity—the effects of Mo addition

Mo doped CoN/CN multilayers show some important features different from those of Co/C and CoN/CN multilayers [29, 30]:

(1) the annealing time needed to approach the *isoconfiguration conditions* is much longer,
(2) the effective interdiffusivities and the macroscopic interdiffusion coefficients are lower and
(3) the activation energy for diffusion is larger.

For amorphous multilayers, the activation energy for diffusion should consist of migration enthalpy and binding enthalpy, which is an intrinsic parameter controlling the interdiffusion process and is strongly associated with the radii of diffusion atoms and chemical binding in sublayers, respectively. The larger activation energy (smaller interdiffusivity) is believed to originate from the strong chemical bonding between Mo and Co, and Mo and N. In order to clarify the chemical bondings, XPS analysis of the CoMoN monolayer was performed to obtain the pure chemical bonding information in the CoMoN sublayers.

The Mo $3d_{5/2}$ peak, as shown in figure 8(a), situated at ∼229.1, 1.1 eV higher than that for the Mo–Mo bond, is partially assigned to the binding energy of the Co–Mo metallic bond. The shift in core-level binding energy has been proved both theoretically and experimentally to depend on the models of the bond formation, such as charge transfer, orbital rehybridization and volume renormalization of atomic energy levels [37–43]. The shift observed here is believed to be associated with charge transfer from the d band of Mo to an unfilled d band of Co. In figure 8(b), the Co $2p_{3/2}$ peak position is at ∼778.02 eV, corresponding to pure cobalt. The shift in core-level binding energy associated with charge transfer is not observed, because the perturbation of Co atoms caused by low-content Mo atoms is too small to be detected. On the other hand, the chemical shift caused by the charge transfer between Co and N was also proved to be hardly seen [30]. Figure 8(c) shows the N_{1s} spectrum, where multi-peak structures are revealed. The peak energy ∼399.03 eV, which is slightly higher than that of nitrogen itself, ∼399.0 eV, is from N≡N bonding. The other two peaks, located at 397.25 and 398.17 eV, respectively, are thought to be associated with the Mo–N and Co–N metallic nitrides, because Mo has a very strong affinity with nitrogen, as evidenced below.

Figures 9(a) and (b) depict the enthalpies of compound formation for the Co–Mo, Co–N and Mo–N systems. It is clear that at any concentrations, the compound formation enthalpy of the Co–Mo system is always negative, and for Co–N and Mo–N systems it is energy favourable (negative) over a certain concentration range. Most obviously, for the Mo–N system, the large negative enthalpy signals Mo has a strong affinity for nitrogen. Therefore they may easily form nitrides during the deposition. This is believed to be the main factor of the significant enhanced incorporation of nitrogen into Co–N films by Mo addition.

Nitrogen incorporates as interstitial atoms in CoMoN layers due to their small radius, and may cause additional shift in Mo_{3d} binding energy. According to the theory of Johansson and

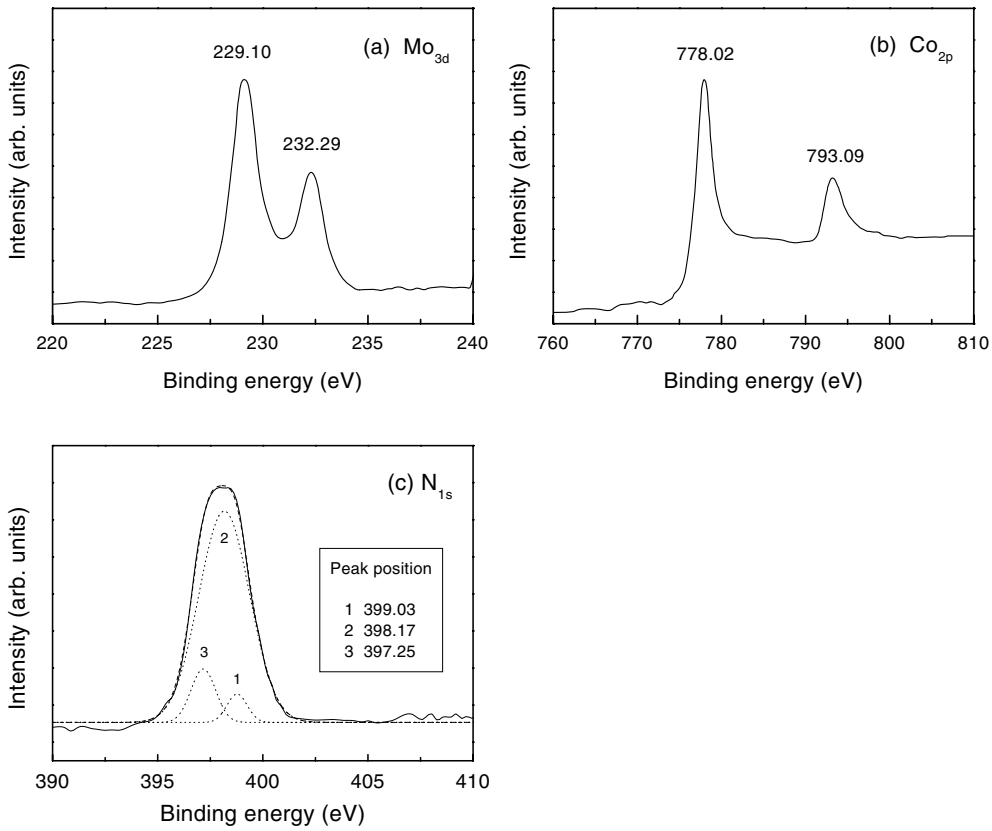

Figure 8. (a) Mo_{3d}, (b) Co_{2p} and (c) N_{1s} XPS spectra.

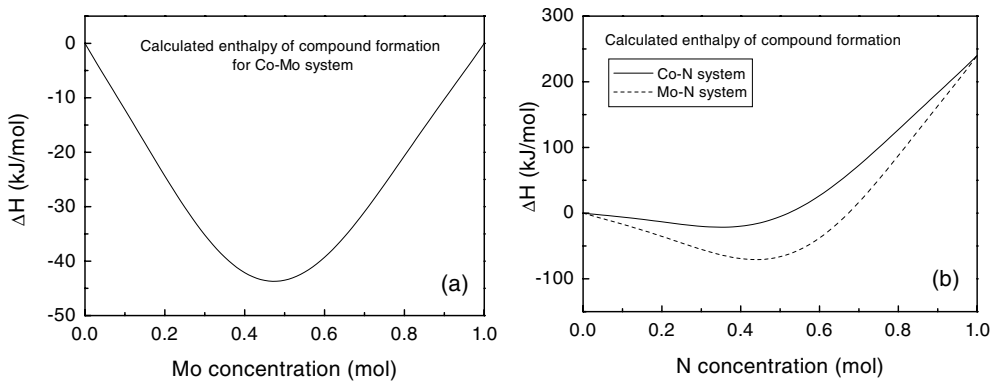

Figure 9. Calculated enthalpy of compound formation for (a) Co–Mo and (b) Co–N and Mo–N systems.

Martensson [44, 45], for the Mo–N system, the chemical shift of Mo can be given as

$$\text{Chemical shift} = -\Delta H_{form}, \tag{11}$$

where ΔH_{form} is the enthalpy of compound formation. The chemical shifts calculated from equation (11) are presented in table 4. One can see that the calculated chemical shift is smaller

Table 4. Calculated enthalpy and chemical shifts of Mo–N compounds.

Compound	MoN	Mo_2N	Mo_3N
ΔH (kJ mol^{-1})	−66.38	−60.47	−45.41
Chemical shift of Mo (eV)	0.69	0.63	0.47

than the experimental value (∼1.1 eV). Apparently, the difference comes from the chemical shift caused by the charge transfer between Co and Mo.

6. Conclusion

CoMoN/CN compound soft-x-ray multilayer mirrors have been fabricated through doping Mo in CoN/CN multilayers by facing-target sputtering. It was found that Mo doping could effectively enhance the incorporation of nitrogen. By investigating quantitatively the interdiffusion in low-temperature annealed CoMoN/CN multilayers at temperatures ranging from 498 to 548 K, we obtained a negative interdiffusivity whose magnitude is smaller than those of Co–C and CoN–CN multilayer systems. The slow back-interdiffusion is believed to be attributable to the strong chemical bonding between Co and Mo, Co (Mo) and N atoms. XPS analyses detected a charge transfer from the valence band of Mo to the unfilled valence band of Co and a remarkable chemical shift of N atoms. Thermodynamic calculations performed based on the Miedema model are well consistent with the experimental analyses. These results suggest that thermally stable interfaces of soft-x-ray optical multilayers can be formed by slight doping with refractory metals.

Acknowledgment

This work is financially supported by the National Science Foundation of China (59801006 and 50172033), Key Teacher Supporting Project, Key Project of Science and Technology and SRF for ROCS for State Education Ministry.

References

[1] Trail J A and Byer R L 1989 *Opt. Lett.* **14** 539
[2] Patrick J, Spiller E and Weisskopf M 1982 *Appl. Phys. Lett.* **40** 25
[3] Stearns D G, Rosen R S and Vernon S P 1993 *Appl. Opt.* **32** 6952
[4] Underwood J H and Barbee T W Jr 1981 *Nature* **294** 429
[5] Finkenthal M, Zwichker A P, Regan S P, Moos H W and Stutman D 1990 *Appl. Opt.* **29** 3467
[6] Ceglio N M, Stearns D G, Gaines D P, Hawryluk A M and Trebes J E 1988 *Opt. Lett.* **13** 108
[7] Spiller E and Golub L 1989 *Appl. Opt.* **28** 2969
[8] Arbaoui M, Barchewitz R, Sella C and Youn K B 1990 *Appl. Opt.* **29** 477
[9] Naguyen T D, Gronscky R and Kortright J B 1990 *Mater. Res. Soc. Symp. Proc.* **187** 95
[10] Stearns D G, Rosen R S and Vernon S P 1990 *Opt. Lett.* **16** 1283
[11] Stearns D G, Rosen R S and Vernon S P 1991 *J. Vac. Sci. Technol.* A **9** 2662
[12] Freitag J M and Clements 2001 *J. Appl. Phys.* **89** 1101
[13] Ravet M F, Bridou F A, Raynal A, Pardo B, Chauvineau J P and André J-M 2001 *J. Appl. Phys.* **89** 1145
[14] Dudás A, Langer G A, Beke D L, Kis-Varga M, Daróczi L and Erdályi Z 1999 *J. Appl. Phys.* **86** 2008
[15] Suresh N, Modi M H, Tripathi P, Lodha G S, Chaudhari S M, Gupta A and Nandedkar R V 2000 *Thin Solid Films* **368** 80
[16] Vitta S and Yang P 2000 *Appl. Phys. Lett.* **77** 3654
[17] Windt D L, Christensen F E, Craig W W, Hailey C, Harrison F A, Jimenez-Garate M, Kalyanaraman R and Mao P H 2000 *J. Appl. Phys.* **88** 460

[18] Agarwal B K 1979 *X-Ray Spectroscopy* (Berlin: Springer) p 134
[19] Cook H E and Hilliard J E 1969 *J. Appl. Phys.* **40** 2191
[20] Mclntyre P C, Wu D T and Nastasi M 1997 *J. Appl. Phys.* **81** 637
[21] Kazama N S and Fujimori H 1983 *J. Magn. Magn. Mater.* **35** 86
[22] Cahn T W 1961 *Acta Metall.* **9** 795
[23] Greer A L and Spaepen F 1985 *Synthetic Modulation Structures* ed L L Chang L L and B C Giessen (New York: Academic) p 424
[24] Steiner P, Hochst H, Steffen W and Hufner H 1980 *Z. Phys.* B **38** 91
[25] Wagner C D, Davis L E, Zeller M V, Tayler J A, Raymond R H and Gale L H 1981 *Surf. Interface Anal.* **3** 211
[26] Sasanuma Y, Uchida M, Okada K, Yamamoto K, Kitano Y and Ishitani A 1991 *Thin Solid Films* **203** 113
[27] Sasanuma Y and Nakayama K 1994 *Thin Solid Films* **247** 24
[28] Bai H L, Jiang E Y, Wang C D and Tian R Y 1997 *J. Appl. Phys.* **82** 2270
[29] Bai H L, Jiang E Y and Wang C D 1996 *Thin Solid Films* **286** 176
[30] Bai H L, Jiang E Y, Wang C D and Tian R Y 1998 *Appl. Phys.* A **66** 423
[31] Setoyama M, Irie M, Ohara H, Tsujioka M, Nomura T and Kitagawa N 1999 *Thin Solid Films* **341** 126
[32] Porter D A and Easterling K E 1981 *Phase Transformations in Metals and Alloys* (Princeton, NJ: Van Nostrand-Reinhold) p 78
[33] Niessen A K and Miedema A R 1983 *Ber. Bunsenges. Phys. Chem.* **87** 717
[34] Lápez J M and Alonso J A 1984 *Phys. Status Solidi* a **85** 423
[35] Miedema A R, de Châtel P H and de Boer F R 1980 *Physica* B **100** 1
[36] Niessen A K, Miedema A R, de Boer F R and Boom R 1988 *Physica* B **151** 401
[37] Rodriguez J A and Goodman D W 1992 *Nature* **257** 897
[38] Rodriguez J A, Campbell R A and Goodman D W 1991 *J. Phys. Chem.* **95** 5716
[39] Rodriguez J A, Campbell R A and Goodman D W 1994 *Surf. Sci.* **303–309** 377
[40] Rainer D R, Corneille J S and Goodman D W 1995 *J. Vac. Sci. Technol.* A **13** 1595
[41] Tikhov M and Bauer E 1990 *Surf. Sci.* **232** 73
[42] Campbell R A, Rodriguez J A and Goodman D W 1991 *Surf. Sci.* **256** 272
[43] He J W, Shea W L, Jiang X and Goodman D W 1990 *J. Vac. Sci. Technol.* A **8** 2435
[44] Johansson B and Martensson N 1980 *Phys. Rev.* B **21** 4427
[45] Steiner P, Hufner S, Martensson N and Johansson M 1981 *Solid State Commun.* **37** 73